

VISUAL ACUITY IN INSECTS

Michael F. Land

Sussex Centre for Neuroscience, School of Biological Sciences, University of Sussex,
Brighton BN1 9QG, United Kingdom

KEY WORDS: vision, eye, optics, acute zone, interommatidial angle

ABSTRACT

The acuity of compound eyes is determined by interommatidial angles, optical quality, and rhabdom dimensions. It is also affected by light levels and speed of movement. In insects, interommatidial angles vary from tens of degrees in Apterygota, to as little as 0.24° in dragonflies. Resolution better than this is not attainable in compound eyes of realistic size. The smaller the interommatidial angle the greater the distance at which objects—prey, predators, or foliage—can be resolved. Insects with different lifestyles have contrasting patterns of interommatidial angle distribution, related to forward flight, capture on the wing, and predation on horizontal surfaces.

INTRODUCTION AND OVERVIEW

Because compound eyes are very different from our own, the question “what can insects see?” has intrigued cartoonists and film-makers as much as entomologists. Since the 1920s, and in particular over the last 25 years, much has been learned about insect visual capabilities, especially their use of colors (including the ultraviolet), their detection of polarized light, and their sensitivity to pattern and motion. However, the groundwork for the study of acuity, the subject of this review, was laid earlier, in the 1890s. Exner’s great monograph of 1892 (13) provided a comprehensive account of the physiological optics of insect eyes. However, it did not define what it is that limits their spatial resolution. This was explained in a brief paper in 1894 by Mallock (46), whose remarkable insights were not properly appreciated for another 60 years.

Mallock was delightfully explicit: “The best of the eyes... would give a picture about as good as if executed in rather coarse wool-work and viewed at a distance of a foot.” In his paper he also explained why insect vision should

be so poor. The problem for compound eyes is that each ommatidium, the receptor unit that samples the image of the surroundings, has its own lens; because there must be a large number of these lenses, they are necessarily small. Mallock realized that the resolution of these tiny lenses is limited by diffraction—a consequence of the wave nature of light that also limits the resolving power of microscopes and telescopes—to about 1° , giving an acuity roughly one hundredth that of the human eye, with its much larger aperture. To give a compound eye the same (about 1 arc-minute) resolution as our eyes would require millions of lenses each as large as a human lens. Such an eye would, he calculated, have a radius of 19 feet (6 m), the size of a large house (for an illustration, see Ref. 30).

Interest in the physical optics of compound eyes began again in the 1950s with de Vries (9) and Barlow (2), and the discussion of the limiting role of diffraction was redeveloped, particularly by Kirschfeld (30) and Snyder (72). In 1941, Hecht et al (see 57) discovered that human vision is limited in dim light by the small numbers of available photons. This limit proved to be just as important for insect vision (58). Another recent discovery is that elongated receptor structures, such as the rhabdoms of compound eyes, behave as waveguides (73). These retain light by internal reflection, but some of the light energy travels outside the structure and can be trapped by external pigment, forming an iris mechanism in many insects (76). By 1980, it is fair to say that the physical principles behind the organization of compound eyes were well understood. These principles were reviewed comprehensively and with authority by Snyder (73).

Over the same period, there were some important discoveries in physiological optics. Exner's division of compound eyes into apposition and superposition types (13) was challenged during the 1960s (22), but this challenge proved misguided (33). The optical and retinal organization in Dipteran flies, where the rhabdomeres of the receptors in each ommatidium are not fused together as in other apposition eyes, was finally solved in 1967 by Kirschfeld (28, 31) and named neural superposition. In 1984, Nilsson et al (51, 52) found that the apposition eyes of butterflies used an optical system that had much in common with the superposition eyes of moths, to which they are closely related. The present state of knowledge on compound eye optics was fully reviewed by Nilsson (49).

With regard to acuity itself, the major refinements since 1950 have been the development of noninvasive methods of measuring acuity using the pseudopupil (15, 23, 76) or ophthalmoscopy (14, 37, 39) rather than the older histological techniques. The main outcome of these have been the realization that most insect eyes have substantial variations in acuity across the eye, reflecting lifestyle and ecology (23, 38). This is a major theme in this review.

THEORETICAL BACKGROUND

Definitions of Acuity: Spatial Frequency

Acuity, in human vision, is defined as the reciprocal of the minimum resolvable angle measured in minutes of arc (89). Usually, this angle refers to that subtended at the eye by two stripes in a grating of equal light and dark stripes, or a similar object. Thus acuity is the reciprocal of a complete period of the pattern, i.e. its “spatial frequency” (ν ; units are cycles per degree or cycles per radian, where $1 \text{ radian} = 180^\circ/\pi = 57.3^\circ$). In this review “acuity” is always used in this sense. An insect’s maximum acuity is referred to as ν_{\max} .

Acuity is sometimes also used to describe the smallest single object that an eye can detect, rather than the finest grating. The physics of these situations are not the same, and single stripes or single objects generally yield much lower angular thresholds. In the old literature, grating and single object thresholds were sometimes referred to as “minimum separable” and “minimum visible.” Here we use “single object threshold” for the latter. The term “resolution” is used in a loose way to mean “ability to resolve fine detail.”

In general, objects such as foliage with complex detail can be thought of as a multitude of gratings with different periods, and the finest detail visible to an insect is determined by acuity (in the strict sense). The better the acuity, the greater the distance at which environmental structures can be used in navigation and locomotory guidance. On the other hand, queen bees sighted by drones against the sky, or insect prey seen on the wing by dragonflies, are examples of small targets for which the single object threshold is a more appropriate guide to performance. Here, good resolution means that small targets can be detected at greater distances.

Features Contributing to an Eye’s Acuity

The performance of any eye is principally affected by three structural and two environmental features. Among the former are (a) the angular spacing of the receptors, which determines how finely an image can be resolved; (b) the quality of the optics (if the image is blurred, then a fine grain retina is wasted); (c) the diameter of the photoreceptors (in a wide receptor—or rhabdom—image detail smaller than its width is lost, and in narrow diameter receptors, waveguide effects also become important). Among the latter are (a) the amount of light available to the receptors (at low light levels there are not enough photons to provide a statistically reliable signal, and the ability to detect contrast declines), and (b) motion (in highly maneuverable animals, such as insects, image motion across the eye causes blur, just as in photography). The following sections will explore these limitations.

This treatment applies strictly to apposition eyes of the type found in diurnal insects such as bees, although many aspects apply to other types of insect eye (neural superposition, afocal apposition, and optical superposition, discussed in detail in a later section). Important differences will be dealt with in a later section. The terminology used here generally follows that of Snyder (73).

Sampling by the Ommatidial Array: Interommatidial Angles

The angle between two detectors in an array is one of the fundamental determinants of acuity (Figure 1a). In a camera-type eye this is the subtense of two receptors at the “nodal point” (the point in the optical system through which rays are not deviated, so that angles in object and image space are the same). In an apposition compound eye, the situation is different because it is the ommatidia rather than the receptors that are the basic sampling units. This is because

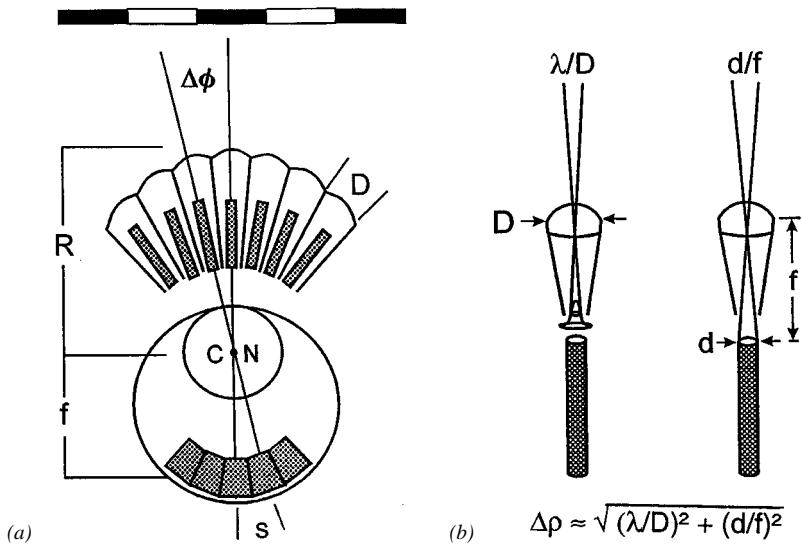


Figure 1 (a) The relationship between acuity in an apposition compound eye (upper) and a simple or camera-type eye (lower). Abbreviations: $\Delta\phi$, angle between receptor units; D , diameter of compound eye facet; R , compound eye radius of curvature; f , focal length of simple eye; s , receptor separation; C , center of curvature of compound eye; N , nodal point of simple eye. Acuity, in both cases, is the angular spatial frequency of the grating (bars at the top of the figure) that the retina can resolve: $1/(2\Delta\phi)$. (Based on 30.) (b) The acceptance angle of an ommatidium ($\Delta\rho$) is a combination of the quality of the optical image, represented by the point-spread function (left) and the rhabdom acceptance angle (right). The way these combine is usually complex, but the equation below gives a useful approximation. Abbreviations: λ , wavelength of light; d , rhabdom diameter; f , focal length of ommatidial optics.

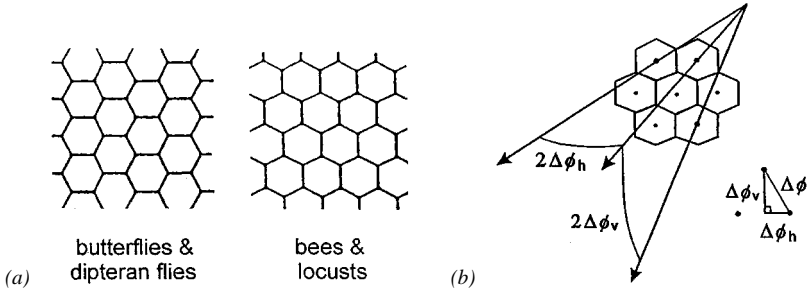


Figure 2 (a) Typical facet patterns with vertical and horizontal rows. (b) Convention for describing the patterns of ommatidial axes (adopted from 76). Insert shows the relationship between the interommatidial angle $\Delta\phi$ and the partial interommatidial angles.

the photodetector, the rhabdom composed of photopigment-bearing microvilli from up to eight receptors, acts as a single light-guide that “scrambles” whatever image reaches its distal tip (Figure 1*b*). There may be spectral or polarization resolution within the rhabdom, but there is no further spatial resolution. As Figure 1*a* shows, in a simple eye the angle between two detectors ($\Delta\phi$) is s/f (rad), where s is the receptor separation and f is the focal length. In an apposition eye the equivalent is the angle between the optical axes of adjacent ommatidia, D/R (rad), where D is the diameter of facet lens and R is the local radius of curvature of the eye.

When an eye views a grating, its composition will be resolved if there are two detectors (receptors or ommatidia) to view each cycle of the grating, one for the dark and one for the light stripe. Finer gratings may be detected but are inaccurately represented (16), a phenomenon known as aliasing. Thus the acuity is set by the sampling frequency of the mosaic (ν_s), where

$$\nu_s = 1/(2\Delta\phi). \quad (1)$$

There is some question as to what is the appropriate interommatidial angle to use when the lattice is hexagonal. In a lattice with hexagons “standing on their tips” as in the eye of a bee, horizontal rows of ommatidial axes are separated vertically by less than the interommatidial angle, specifically $(3)^{1/2}\Delta\phi/2$ (Figure 2*a*). Some argue that this, rather than $\Delta\phi$ itself, is the proper basis for measuring acuity in some circumstances (73, 76), but the evidence is equivocal. Here we will use the simple interommatidial angle $\Delta\phi$ wherever possible. Figure 2*b* shows a useful scheme introduced by Stavenga (76) that uses the partial interommatidial angles ($\Delta\phi_h$ and $\Delta\phi_v$) to define a rectangular matrix that fully describes the hexagonal pattern. This scheme can describe all types of sampling mosaics, including ones whose form changes across the eye. A difficulty with

the Stavenga scheme is that one or other of the partial interommatidial angles is equal to $\Delta\phi/2$, which can be confusing. Horridge (23), for example, uses twice the values of $\Delta\phi_h$ and $\Delta\phi_v$, as horizontal and vertical interommatidial angles. Readers should be aware of such differences in usage.

The acuity indicated by the sampling frequency (Equation 1) will only limit resolution if the ommatidial optics are good enough to resolve this spatial frequency, or better. We now consider how optical factors limit acuity.

Optical Quality

As the detail in an object gets finer, the contrast in its image decreases until at some point it becomes zero (Figure 3*b*). Above this spatial frequency there is

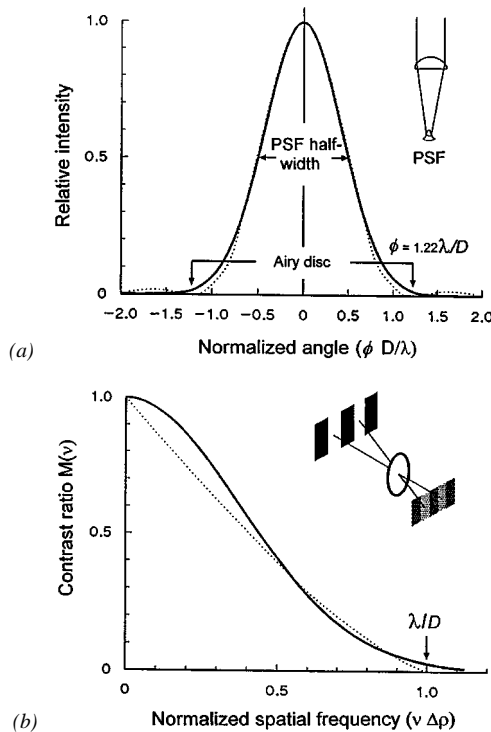


Figure 3 (a) Luminance distribution in the image of a point-source object (the point-spread function, PSF; see insert). Dotted line is the Airy diffraction pattern, showing the position of the first dark ring, and solid line is the Gaussian approximation. ϕ is angle in image space; other abbreviations as in Figure 1. (b) Modulation transfer function, $M(\nu)$, corresponding to the point-spread function shown in (a). Insert shows the contrast reduction in the image formed by a lens. Abbreviations: ν , angular spatial frequency of object; $\Delta\rho$, acceptance angle (see Figure 1*b*).

nothing left to detect. All optical systems have such a cut-off frequency. The fundamental reason for this is diffraction (see below), although other imperfections such as focus defects can also blur the image, i.e. prevent high spatial frequencies from reaching it. The existence of a cut-off frequency means that there is an upper useful limit to the sampling frequency (ν_s) of the mosaic. If the cut-off frequency is ν_{co} , then the maximum possible resolution is achieved when the mosaic can just resolve the image that the optics are just capable of providing, in other words

$$\nu_{co} = \nu_s = 1/(2\Delta\phi). \quad (2)$$

In the human eye, in daylight, this condition is almost exactly met: ν_s and ν_{co} are both close to 60 cycles per degree. In insects the available evidence suggests that ν_s is closer to $\nu_{co}/2$ (39, 87), meaning that the image provides the receptors with a reasonable amount of contrast, compared with the near zero contrast that the human retina is able to respond or perceive at the resolution limit.

THE DIFFRACTION LIMIT If the optics are otherwise free of defects, the limit to resolution is set by diffraction. The image of a point object is not a point but a diffraction pattern known as the Airy disc (Figures 1*b*, 3*a*). This has a central intensity maximum outside of which are a series of rings of minima and maxima of sharply decreasing intensity. The wider the lens aperture (D), the narrower the Airy disc, and hence the finer the resolution in the image. The most convenient measure of the pattern is the width of the central bright disc at half maximum intensity (the half-width), which is almost exactly λ/D radians (Figure 3*a*), where λ is the wavelength of light (500 nm for blue-green light) (73). The distribution of light in the image of a point source is also known as the point-spread function (PSF), which may be wider than the Airy disc because of other optical imperfections but can never be narrower. One can think of this as the blurring function in the conversion of object to image. This blurring will have little effect on coarse gratings, but as the grating period approaches the half-width of the PSF, the contrast in the image declines, and it finally reaches zero at the cut-off frequency (ν_{co}). In a diffraction limited eye, this frequency is equal to the reciprocal of the point-spread function half-width (hw). Thus

$$hw_{\text{PSF}} = \lambda/D, \quad (3)$$

and

$$\nu_{co} = D/\lambda \quad (4)$$

MODULATION TRANSFER FUNCTION A convenient description of the performance of an eye's optics is given by their modulation transfer function (MTF). This gives the ratio of the image and object contrasts for gratings of all spatial frequencies. Contrast is defined as $(I_{\max} - I_{\min}) / (I_{\max} + I_{\min})$, where I_{\max} and I_{\min} are the maximum and minimum intensities in the object or image. For a diffraction limited but otherwise defect-free lens the MTF has the form shown in Figure 3*b*. The graph shows that the image contrast declines almost linearly from 1 (for very coarse gratings) to 0 (at the cut-off frequency). Lenses that are defocused or have aberrations of various kinds show more complicated MTFs, but in general the optical systems of both well-focused human eyes and unfocused insect eyes behave more or less like that shown in Figure 3*b*. The MTF and the PSF can be derived from each other mathematically (37, 73).

Effect of Rhabdom Diameter

Each rhabdom picks off a small portion of the total image (Figure 1). If the rhabdom is narrower than the image of a single stripe, it will faithfully report the intensity of the stripe imaged on it. However, if the rhabdom is wider than this, it will swallow however many stripes fit into its diameter. In camera-type and optical superposition eyes this is not a problem because the receptors are contiguous. In apposition eyes, however, there is no real restriction on receptor width, especially in dark-adapted eyes where the rhabdoms can swell to two or more times their diurnal diameter as they seek to capture more light (88). This inevitably compromises resolution.

Even the narrowest rhabdoms ($< 2 \mu\text{m}$) fail to act as perfect "point detectors," behaving as though they have diameters greater than their actual width. Light forms interference patterns within narrow light-guiding structures, and these patterns are known as waveguide modes (71, 73). The so-called fundamental mode, which is the only one present in the narrowest rhabdoms or receptors, has a substantial fraction of its energy outside the boundaries of the structure that guides it. This has two consequences. In apposition eyes it means that narrow rhabdoms always appear to have a diameter rather larger than their real diameter, compromising resolution slightly. In eyes with contiguous receptors this leakage means that light energy from one receptor can find its way into its neighbors, again spoiling resolution. This gives a practical lower limit to receptor diameter of 1–2 μm .

The number of modes present, and the amount of energy in each mode, is determined by the waveguide parameter V , which in turn is determined by the rhabdom diameter, the refractive index difference between the rhabdom (n_r) and its surroundings (n_s), and the wavelength of light.

$$V = \frac{\pi d \sqrt{(n_r^2 - n_s^2)}}{\lambda} \quad (5)$$

If any of these parameters change, the mode pattern changes, and so does the apparent diameter of the rhabdom. These effects are not large, but they are measurable (43, 70).

In wider rhabdoms more waveguide modes are supported. Eventually, when the guiding structures are 5–10 μm wide, the sum of all these modes becomes indistinguishable from what geometrical optics and simple anatomy would predict: The rhabdom accepts light only over its actual cross section, and light is held within it by total internal reflection.

Angular Sensitivity and Acceptance Angle

The combined effect of optical blurring by the lens, the width of the rhabdom, and the waveguide modes it contains is not simple to calculate. However, this has been done (53, 54, 78, 79), and the results accurately predict the measured angular sensitivities of the retinal receptors (17, 70).

For many purposes, an approximation by Snyder (73) greatly simplifies the problem of combining the two blurring functions. If we assume that both the point-spread function and rhabdom acceptance function are Gaussian in profile, which is usually more or less the case, then their half-widths (hw) add as follows:

$$hw_{\text{comb}}^2 = hw_{\text{lens}}^2 + hw_{\text{rhab}}^2, \quad (6)$$

where *comb*, *lens*, and *rhab* refer to the combination, the PSF of the lens, and the acceptance function of the rhabdom respectively. For rhabdoms wider than a few micrometers, the acceptance function can be taken to have a half-width equal to the rhabdom diameter, which in angular terms is given by d/f (Figure 1*b*). The Airy disc half-width is given by λ/D , where D is the lens diameter. Thus the half-width of the rhabdom's angular sensitivity, usually referred to as the ommatidial acceptance angle $\Delta\rho$, can be obtained from the following:

$$\Delta\rho = \sqrt{(d/f)^2 + (\lambda/D)^2}. \quad (7)$$

The effective cut-off frequency of the whole optical system including the rhabdom (ν_{opt}) is then given by

$$\nu_{\text{opt}} = 1/\Delta\rho. \quad (8)$$

Equation 7 works well for wider rhabdoms, but tends to overestimate $\Delta\rho$ by up to 30% in eyes with narrow rhabdoms or rhabdomeres that support only one or two modes. In the fly *Calliphora erythrocephala*, Equation 7 predicts a value for $\Delta\rho$ of 1.83° for receptors 1–6, whereas a method that takes account of the optical coupling of the lens diffraction pattern to the waveguide modes

of the rhabdomeres predicts a value of 1.24° (78). The problem is discussed by van Hateren (78, 79).

If the acceptance function is approximately Gaussian with a half-width $\Delta\rho$, then the MTF of the receptors is given by the following:

$$M(\nu) = e^{-3.56(\nu\Delta\rho)^2}. \quad (9)$$

where $M(\nu)$ is the contrast ratio at spatial frequency ν (Ref. 73, p. 235), (Figure 3b).

Photons, Sensitivity, and Resolution

At low light levels, photons enter receptors at a very low rate. At the absolute human threshold, each receptor receives 1 photon on average every 40 minutes (57), and the situation in insects is similar (58).

Small numbers mean poor statistics. In the case of light we are lucky because the nature of the statistical variation is well understood. Small numbers of events sampled from a large pool obey Poisson statistics, and one feature of this kind of distribution is that the variance is equal to the mean (56, 57, 59). A result that is not hard to derive from this is that low contrasts require very large numbers of photons for their detection. It can be shown (36, 59) that the average number of photons per receptor \bar{N} needed to detect a grating of contrast C is given by the following:

$$\bar{N} > 1/C^2. \quad (10)$$

If the contrast in a grating is 0.5, the number required is $1/0.5^2 = 4$. With a contrast of 0.1, the number is 100, but when the contrast is down to 0.01, the number is 10,000. The integration time of most insect receptors is considerably less than 0.1 s (25), so at low contrast each receptor would require photon numbers approaching a million, and these are only available at daylight light levels.

A related effect of low photon numbers is to limit acuity by placing a lower limit to the usable contrast in the MTF (Figure 3b). Thus with 10 photons per integration time available, the contrast limit will be 0.32, and that will limit the maximum spatial frequency to about 60% of the cut-off frequency.

In view of these limitations, it is important to know how many photons are actually available to receptors under different lighting conditions. This is given, approximately, by the following expression (29, 36):

$$N = 0.62ID^2d^2/f^2, \quad (11)$$

where d , D , and f have their usual meanings (Figure 1) and I is the luminance of the source being imaged, expressed as photons per unit area per steradian per

second (if the area chosen is 1 m^2 , then D must also be expressed in meters). The expression d/f is also the geometrical acceptance angle ($\Delta\rho$ in Equation 7, ignoring diffraction, as is appropriate in the case of an extended source), so $\Delta\rho^2$ can replace d^2/f^2 in Equation 11.

AVAILABLE PHOTON NUMBERS A white card in bright sunlight emits about 10^{20} photons $\text{m}^{-2} \text{sr}^{-1} \text{s}^{-1}$, about 10^{17} in room light, 10^{14} in moonlight, and 10^{10} in starlight—the absolute threshold for human vision (36). When using the eye dimensions for a diurnal insect ($D = 25 \mu\text{m}$; $d = 2 \mu\text{m}$; $f = 60 \mu\text{m}$), Equation 11 yields photon numbers per receptor per second of $4 \cdot 10^7$ for sunlight, $4 \cdot 10^4$ for roomlight, 40 for moonlight, and 0.004 (1 every 4 minutes) in starlight. These reduce by perhaps another 2 log units when the receptor integration time [10–50 milliseconds (ms), Ref. 25], transmission losses, and the quantum efficiency of transduction (56) are taken into account. It is then clear that resolution will be always compromised in illumination conditions dimmer than roomlight. Diurnal insects do not fly in light levels lower than this.

ADAPTATIONS TO DIM LIGHT Many insects are crepuscular. Moths and beetles particularly, but some dragonflies [*Zyxomma obtusum* (23)], butterflies [*Melanitis sp. leda* (43)] and many Diptera fly at light levels between those of roomlight and moonlight. The kinds of adaptations (other than dark adaptation at the receptor level) that make flight possible under these conditions follow from Equation 11. In apposition eyes, wider facets (D) and wider rhabdoms (d) can increase sensitivity by 1–2 log units (88). Receptor integration time may increase up to fivefold in the dark (25). The optical arrangements in moths and some beetles (optical superposition) and in Dipteran flies (neural superposition) are also specializations that increase the available photon numbers in dim light (see Figure 4).

Effects of Motion on Resolution

Because of the photoreceptors' finite integration time, the retinal image is subject to motion blur when eye and surroundings move relative to each other. As a rule of thumb, the image will start to lose contrast at high spatial frequency when the relative motion exceeds one acceptance angle ($\Delta\rho$) per receptor integration time (Δt) (41). Δt can be defined as the half-width (in time) of the response to a small flash of light, and in most insects this is in the range of 5–50 ms (25, 45). Thus if an insect has $\Delta\rho = 1^\circ$ and $\Delta t = 20 \text{ ms}$, then blur will occur at angular velocities greater than 50° s^{-1} . In high-speed manoeuvres, insects can rotate at speeds up to several thousand degrees per second (7, 40) and routinely turn at speeds well into the hundreds of degrees per second, so blurring is a real problem.

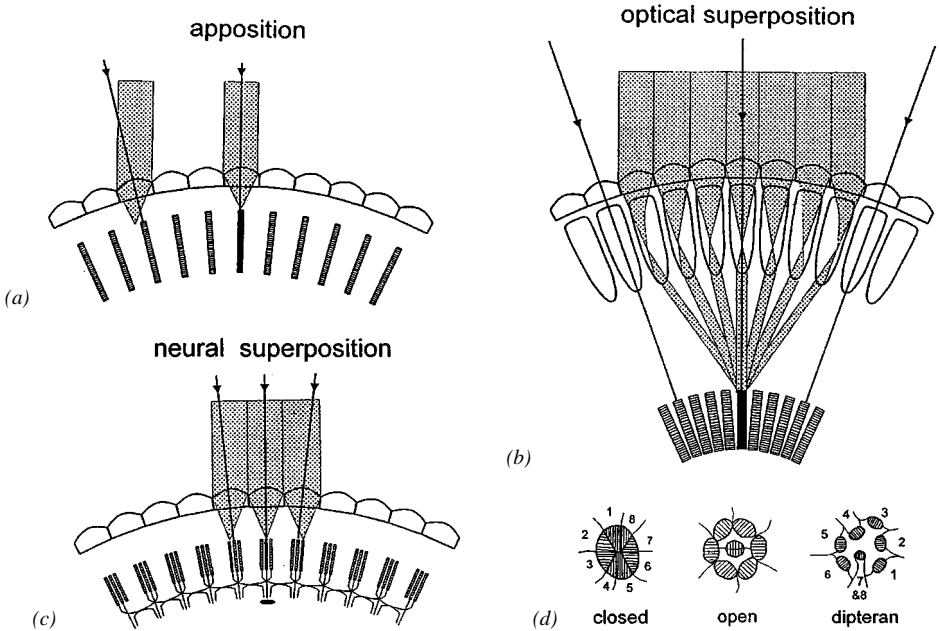


Figure 4 Image formation in different types of compound eye. Stippled beams show the light contributing to the neural signal from the image of a distant point (the apposition eye also shows a beam from the same source that does not contribute to the signal). Illuminated rhabdoms, or rhabdomeres in (c), shown in black. Arrowed lines are axes of individual ommatidia. (d) Patterns of receptor contributions to the rhabdoms of a bee (closed), a hemipteran (open), and a fly. Numerals show conventional receptor numbering.

Snyder (73) estimated the effects of motion blur in terms of the increase in width of the acceptance function $\Delta\rho$. He used a similar Gaussian approximation to that in Equations 6 and 7 to derive the extended acceptance angle ($\Delta\rho$). If the angular velocity across the retina is v , then

$$\Delta\rho_v^2 = \Delta\rho^2 + (v\Delta t)^2. \tag{12}$$

The effect on the MTF, which will be reduction of contrast at the higher spatial frequencies, can be obtained from Equation 9, substituting $\Delta\rho_v$ for $\Delta\rho$.

Resolution and Eye Size

The multi-lens design of compound eyes has dire consequences when there is a need for high resolution (30, 44). The reason is that small lenses are diffraction limited, and so to increase resolution by a factor of two, for example, requires a doubling of the diameter of each ommatidium as well as a doubling of the

number of ommatidia in a row. The consequence is that the eye must grow as the square of the required acuity. To achieve vertebrate-like acuity, the eye would need to be huge.

In a diffraction limited compound eye, $v_{co} = v_s$. Substituting from Equations 1 and 4 gives $D/\lambda = 1/(2\Delta\phi)$. But $\Delta\phi = D/R$ (Figure 1), where R is the eye radius, so that substituting for D gives $R\Delta\phi/\lambda = 1/(2\Delta\phi)$, or

$$R = \lambda/(2\Delta\phi^2) = 2\lambda v_s^2. \quad (13)$$

If the interommatidial angle is 1° (0.0175 rad), typical of insects, then for a wavelength λ of $0.5 \mu\text{m}$ this equation predicts an eye radius of 0.82 mm, which is reasonable enough, but if we make $\Delta\phi$ equal to 0.5 minutes (0.00015 rad), the spacing of cones in the human fovea, then the eye radius becomes 11.7 meters! In fact the largest insect eyes, those of dragonflies, have interommatidial angles of about 0.25° . In general, the only realistic way that a compound eye can achieve resolution much better than a degree is to build in an “acute zone”—a small region with larger facets and higher acuity (23, 38). We shall see that this is a very common strategy.

A second consequence of the diffraction limit is that it predicts a square root relationship between ommatidial diameter and eye size (2, 46). Substituting D/R for $\Delta\phi$ in $D/\lambda = 1/(2\Delta\phi)$ gives $D = (R\lambda/2)^{1/2}$. Barlow (2) found that ommatidial diameter was indeed proportional to the square root of eye size over a wide range in Hymenoptera.

Acuity of Other Types of Compound Eye

In apposition eyes, each rhabdom has its own lens, and the rhabdoms themselves are “fused,” with the contributions of the receptors forming a single light-guiding structure (Figures 4a, 4d). There are three important variants of this structure: “open rhabdom” or “neural superposition,” “optical superposition,” and “afocal apposition.”

Dipteran flies have eyes that are optically of the apposition type, but the photoreceptors of each ommatidium keep their individual photoreceptive structures (rhabdomeres) separated by $1\text{--}2 \mu\text{m}$. Thus in the image plane there are seven separated receptive structures (Figures 4c, 4d). Evidently the image within each ommatidium is partially resolved. What, then, is the relationship between these resolved inverted images and the overall erect image? Although the open rhabdom structure was described last century, this question was not finally resolved until the 1960s. Kirschfeld (28, 31) showed that the central rhabdomere in one ommatidium shares a field of view with one of the rhabdomeres in each of six adjacent ommatidia. Furthermore, all the receptors that thereby image the same direction in space send their axons, via a complex crossover arrangement, to the same synaptic “cartridge” in the lamina, hence

the name neural superposition. For this to work the angular separation of rhabdomeres (s/f) has to be the same as the interommatidial angle ($\Delta\phi = D/R$) across the whole eye. The attainment of this apparently complicated arrangement permits the pooling, in the lamina, of the photon signals of 7 receptors, and hence a $\sqrt{7}$ improvement in contrast detectability (Equation 10), without compromising resolution. In a conventional apposition eye this would require an increase in rhabdom diameter (by $\sqrt{7}$) which in turn would both increase the receptor acceptance angle ($\Delta\rho$) and decrease resolution. The result of this extra sensitivity is an extension of activity of about 15 minutes at sunrise and sunset; although this may not seem like much, it is in these brief spells that the insects can see well enough to swarm and mate, while their avian predators struggle to see them. The origins of this kind of eye are discussed by Nilsson & Ro (50).

The optical superposition eyes of moths and nocturnal beetles are of a quite different construction (Figure 4*b*). Exner (13) discovered that many facets of these eyes contributed to a single, real, deep-lying, erect image. He also worked out that for this to happen, the optical elements had to have the properties of two-lens telescopes rather than simple lenses, and that these telescopic elements could only achieve their optical power from an internal gradient of refractive index. These ideas have turned out to be completely correct (6, 33).

Optically, this type of eye needs to be treated more like a simple (camera-type) eye because of its single image (Figure 4*b*). From the eye's geometry, its focal length is the distance out from the center of curvature to the image, typically about half the radius of curvature of the eye. The interreceptor angle ($\Delta\phi$, radians) is then the receptor separation divided by the focal length. Usually, this is in the same range ($1-5^\circ$) as in apposition eyes, and acceptance angles ($\Delta\rho$) are also similar. The real difference comes in sensitivity: The effective aperture (D) is no longer the width of a single facet but is ten facets or more. This increases the sensitivity by 1-3 log units (Equation 11), allowing insects such as moths and beetles, including fireflies, to forage and mate late into the evening.

The eyes of butterflies have telescopic optical elements like optical superposition eyes, but the rhabdoms are close to the proximal end of these structures (the crystalline cones), as in apposition eyes, and each rhabdom views the world through only a single lens (51, 52). These eyes are referred to as afocal because light from a distant point emerges as a parallel beam rather than a focused spot, and the acceptance angle $\Delta\rho$ is set by the critical angle for internal reflection in the rhabdom, rather than its diameter. However, in practice they are very similar in performance to ordinary (focal) apposition eyes. They may in fact be very slightly superior in terms of resolution because the rhabdom waveguide modes couple better to the output of the optical system (80).

METHODS OF MEASURING ACUITY

Interommatidial Angles ($\Delta\phi$)

In principle the measurement of $\Delta\phi$ should be simple. If a row of ommatidia subtending 90° in space is 45 facets long, then the average interommatidial angle must be 2° . The problem is that the optical axes of ommatidia are rarely aligned exactly perpendicular to the eye surface, and so overall estimates based on external measurements tend to miss important features such as acute zones.

Some global measurements can give useful average results, however. An insect eye that covers 180° of space has a total field of view containing 20,626 square degrees (a solid angle 1° high and 1° wide). A hexagonal field of view covers $0.866\Delta\phi^2$ square degrees, where $\Delta\phi^\circ$ is the angular separation of centers of the hexagons. Thus the number (n) of ommatidial fields of view that can cover a hemisphere, without overlap is $23818/\Delta\phi^2$ or $\Delta\phi = (23,818/n)^{1/2}$. In *Musca domestica* (having 3000 ommatidia) $\Delta\phi$ comes to 2.8° , and in *Drosophila melanogaster* (having 700 ommatidia) $\Delta\phi$ comes to 5.8° . Both estimates are close to measured values.

Before the 1960s, $\Delta\phi$ was commonly measured from histological sections, and when properly interpreted, these gave accurate results (3, 10). They demonstrated variations in $\Delta\phi$ across the eye in bees and butterflies, as well as differences between vertical and horizontal angles. However, differential tissue shrinkage always remained a likely source of error.

More recently, measurements of $\Delta\phi$ have involved the use of the pseudopupil in its various forms. The pseudopupil, typically a black dot that appears to move around the insect's eye as the observer's viewpoint changes, marks the ommatidia that image—and absorb light from—the observer. Thus a line joining the pseudopupil to the observer's eye is the direction of view of the ommatidia in that region. Local measurements of $\Delta\phi$ can be made easily by rotating the eye through a known small angle (a) and counting the number of ommatidia (b) crossed by the pseudopupil, $\Delta\phi$ is then a/b . Typically, measurements are made with the animal centered on a goniometric stage, and the pseudopupil is observed or photographed through a microscope (23). Where the interommatidial angles are small, as for example in the acute zones of dragonfly eyes, the best pseudopupil image lies some distance below the cornea (the deep pseudopupil), and it is important to use a small microscope aperture so that both cornea and pseudopupil can be visualized together. Because the pseudopupil is actually a magnified image of both the rhabdom and its surrounding pigment, its center must be located to find the ommatidial axis direction. Usually this is not a problem, but where interommatidial angles change rapidly, the pseudopupil becomes asymmetric and care is required.

In dark colored eyes the pseudopupil is often not apparent. Crossed polarizing fibers can be used to cut down reflections, but a more generally useful technique is known as the antidromic pseudopupil (15). Here the center of the head is illuminated from below, and light finding its way into the proximal part of the rhabdom(ere)s is emitted from their distal tips. This produces a luminous pseudopupil, which can be examined in the same way as the dark "orthodromic" kind. Pseudopupil methods are discussed and reviewed in references (14, 23, 76, 87).

The final method of determining $\Delta\phi$ is to measure ν_s behaviorally, and assume that $\nu_s = 1/(2\Delta\phi)$ (Equation 1). This method uses the optokinetic response, in which an insect at the center of a striped drum will turn with the drum to minimize the displacement of the image across the retina. If the grating is of high contrast and brightly illuminated, then the finest grating that can be detected should coincide with the sampling frequency. Important early studies included the beetle *Chlorophanus viridis* (20) and the fly *Drosophila melanogaster* (16). Comparing the behavioral results with values for $\Delta\phi$ obtained from anatomical measurements, Wehner (87) commented: "These numbers, being accurate to half a degree, all agree well with the half-periods of the highest frequency gratings resolved by the species. To my knowledge, there is no single insect or crustacean species in which this correspondence has not been confirmed whenever the experimental conditions have been selected carefully enough." This gives us confidence that the values of $\Delta\phi$ measured by anatomical and optical methods are indeed those of relevance to the insects.

Srinivasan & Lehrer (75) used a different behavioral method in honeybees, training them to distinguish gratings with vertical and horizontal stripes at different distances. They found that the highest spatial frequency reliably resolved by the bees was $0.26 \text{ cycle deg}^{-1}$, with no evidence of a difference in acuity between horizontal and vertical gratings. This grating has a half-period of 1.9° , which is considerably less than the horizontal interommatidial angle ($2\Delta\phi_h$), which has a minimum of 2.8° (38, 67). This implies that in this case the ommatidia detecting the gratings are arranged in obliquely alternating vertical rows (see Figure 2).

Acceptance Angles ($\Delta\rho$)

Electrophysiological recordings from single insect receptors have been made since the 1960s. By giving flashes from a small light source as it moves through the center of a cell's receptive field, the angular acceptance function of that cell can be built up. $\Delta\rho$ is then the width of the function at half maximum sensitivity. Early estimates of $\Delta\rho$ that used this method tended to be overestimates because of damage, and it was not until the 1970s that the technique was perfected (17). However, since then theoretical (Equation 7) and measured values for

$\Delta\rho$ have come into agreement for a number of species (see Table 2). A recent improvement of the method is the use of a “light-clamp” in which the receptor’s response is kept constant by the use of a density wedge in a feedback loop (70).

It is often possible to use an optical method to make the angular acceptance function visible as an intensity field outside the eye. The technique involves illuminating the eye so that light emerges from the distal tip of the rhabdom, either using antidromic illumination from behind the retina (14) or light reflected back from a tapetum (37, 52). This light can be collected and imaged by a suitable optical system, and its distribution measured. The principle of the reversibility of light implies that the light emitted by the rhabdom should have the same distribution as the light accepted, so that the half-width of the emitted light should equal $\Delta\rho$. In the blowfly *Calliphora erythrocephala*, this method gave minimal values for $\Delta\rho$ of 1.24° (78), essentially identical to the electrophysiological measurements (17, 70) and in perfect agreement with calculations that used appropriate waveguide theory.

RESULTS OF ACUITY MEASUREMENTS

Differences Between Insect Groups

Table 1 gives a list of reliable measurements of interommatidial angle in insects classified by order and by eye type. Unless otherwise indicated, these are minimum values from the front part of the eye. Where vertical and horizontal angles differ, as they often do, the compromise angle [$\Delta\phi = (\Delta\phi_h^2 + \Delta\phi_v^2)^{1/2}$; see Figure 2*b*] is used. Other things being equal, one would expect acuity to be close to $1/(2\Delta\phi)$.

The angle $\Delta\phi$ varies from tens of degrees in Collembola to 0.24° in the acute zone of the dragonfly *Anax junius*, roughly in line with the sizes of these animals’ eyes. Many common flying insects—e.g. bees, flies, and butterflies—have $\Delta\phi$ in the range $1\text{--}3^\circ$, predicted from their eye diameters of around 1 mm (Equation 13). Most insects with $\Delta\phi$ less than 1° are predators—dragonflies, mantids, and sphecid wasps—and in all cases the value quoted comes from the forward-pointing region of the acute zone used for tracking prey. In many Diptera, however, and in some other orders, only the male has a high acuity region, which is used to detect and pursue females (see section on forward flight pattern). In some insects the eyes are actually double, e.g. in mayflies, the neuropteran owl flies *Ascalaphus macaronius*, and the nematoceran fly *Bibio marci*. The upward-pointing dorsal eye always has the higher resolution and is used for detecting females or prey against the sky (32, 90). There seem to be no obvious differences in acuity between the different types of eye; among

Table 1 Minimum interommatidial angles for insect species ^a

Order	Species	Eye Type	$\Delta\phi$	Method	Ref.
Apterygota					
Collembola	<i>Dicyrtomina ornata</i>	A	25–57°	A	55
Pterygota					
Ephemeroptera	<i>Ephemera vulgata</i>	A?	2.2°	A	48
	<i>Atelophlebia</i> sp. ♂	(D) OS? (V) A?	2.0° 3.3°	A A	24 24
Odonata	<i>Anax junius</i>	A	0.24°	P	69
	<i>Sympetrum striolatum</i>	(D) A (V) A	0.4° 1.8°	P P	35 35
	<i>Austrogomphus guerini</i>	A	0.58°*	P	23
	<i>Zygomma obtusum</i>	A	0.65°*	P	23
	<i>Aeschna grandis</i>	A	0.8°	A	48
	<i>Xanthagrion erythroneurum</i>	A	1.2°*	P	23
	<i>Orthoptera Locusta migratoria</i>	A	0.9°*	P	23
Phasmida	<i>Dixippus morosus</i>	A	7.5°	A	48
Dermaptera	<i>Forficula auricularia</i>	OR	7.2°	P	50
	Dictyoptera				
	<i>Tenodera australasiae</i>	A	0.6–2.5°	P	60
	<i>Orthodera ministralis</i>	A	1.2°*	P	23
	<i>Cuifina</i> sp.	A	0.8°*	P	23
	<i>Gerris paludum</i>	OR	2.1°*	P	8
Hemiptera	<i>Notonecta glauca</i>	OR	1.65°*	P	65
	<i>Sialis flavilatera</i>	A?	2.4°	A	48
Neuroptera	<i>Ascalaphus</i> sp.	(D) OS	1.4°	A	64
	<i>Ascalaphus</i> sp.	(V) OS	2.0°	A	64
	<i>Cicindela hybrida</i>	A	1.5°	A	48
Coleoptera	<i>Anoplognathus pallidicollis</i>	OS	1.5°	A,P	85
	<i>Cantharis livida</i>	A	1.8°	A	48
	<i>Photurus versicolor</i>	OS	1.8°	A	22
	<i>Onitis alexis</i>	OS	2.5°	A	85

(Continued)

Table 1 (Continued)

Order	Species	Eye Type	$\Delta\phi$	Method	Ref.	
	<i>Coccinella</i>					
	<i>septempunctata</i>	A	2.9°	A	83	
	<i>Chrysomela fastuosa</i>	A	5.4°	A	83	
	<i>Zophobas morio</i>	OR	5.9°	P	50	
	<i>Lixus blakeae</i>	A	6°	AB	87	
	<i>Tenebrio molitor</i>	A	6.5°	AB	87	
	<i>Chlorophanus</i>					
	<i>viridis</i>	A	7°	AB	87	
	<i>Phyllobius urticae</i>	AA	7°	A	83	
Lepidoptera	<i>Papilio macaon</i>	AA	0.9°	A	48	
	<i>Heteronympha merope</i>	AA	1.4–2.6°	P	39	
	<i>Pieris brassicae</i>	AA	1.8°	A	83	
	<i>Phalaenoides</i>					
	<i>tristifica</i>	OS	1.9°	O	37	
	<i>Ocybadistes walkeri</i>	OS	2.0°	O	37	
	<i>Ephestia kühniella</i>	OS	3°	A	6	
Diptera	<i>Syrirta pipiens</i>	♂	NS	0.6°	P	7
			NS	1.5°	P	7
	<i>E. tenax</i> ♂		NS	1°	A	48
	<i>Calliphora</i>	♂				
	<i>erythrocephala</i>		NS	1.1°	P	42
			NS	1.3°	P	42
	<i>Bibio marci</i> ♂	(D)	NS	1.6°	P	90
		(V)	NS	3.7°	P	90
	<i>Musca domestica</i>	NS	2.5°	APB	87	
	<i>Drosophila</i>					
	<i>melanogaster</i>	NS	5°	APB	87	
Hymenoptera	<i>Tipula pruinosa</i>	OR	5.8°	P	50	
	<i>Bembix palmata</i>	A	0.41°*	P	23	
	<i>Apis mellifera</i>	♂	A	0.8°	A	48
		worker	A	1°	APB	87
			A	1.3°	A	48
	<i>Amegilla</i> sp.	A	1°*	P	23	
	<i>Vespa vulgaris</i>	A	1°	A	48	
	<i>Myrmecia gulosa</i>	A	1.7°	P	84	
	<i>Cataglyphis bicolor</i>	A	4°	P	92	

^a(D) dorsal eye; (V) ventral eye. Eye type: A, apposition; AA, afocal apposition; NS, superposition; OR, open rhabdom; OS, optical superposition; ?, uncertain. Methods: A, anatomy; B, behaviour; O, ophthalmoscopy; P, pseudopupil. * indicates a value derived from data in the reference, usually by calculating $\Delta\phi$ as $(\Delta\phi_n^2 + \Delta\phi_r^2)^{1/2}$.

Table 2 Comparisons of interommatidial ($\Delta\phi$) and acceptance ($\Delta\rho$) angles

Species	Eye Type	$\Delta\phi$	$\Delta\rho$	$\Delta\rho/\Delta\phi$	Method	Ref.
<i>Hemicordulia tau</i>	A	0.9°	1.4°	1.56	PE	44
<i>Tenodera</i>						
<i>australasiae</i> front	A (LA)	0.6°	0.7°	1.17	PE	60
	(DA)		2°	3.3		
edge	(LA)	2.5°	2.5°	1.0		
	(DA)		6°	2.4		
<i>Anoplognathus pallidicollis</i>	OS (LA)	1.5°	3°	2	AE	85
	(DA)		5°	3.3		
<i>Onitis alexis</i>	OS	2.5°	4.3°	1.72	AE	85
<i>Heteronympha merope</i>	AA (LA)	1.25°	1.5°	1.2	PO	39
	(DA)		2.0°	1.6		
<i>Melanitis leda</i>	AA (LA)	1.44°	1.5°	1.04	PO	39
	(DA)		2.7°	1.88		
<i>Phalaenoides</i>						
<i>tristifica</i>	OS	1.9°	1.58°	0.83	O	37
<i>Ocybadistes walkeri</i>	OS	1.95°	2.18°	1.12	O	37
<i>Calliphora</i>						
<i>erythrocephala</i>	NS					
(R1-6) front	(LA)	1.5° (a)	1.02° (b)	0.68	PE	42(a)
	(DA)		1.22° (b)	0.81		70(b)
ventral	(LA)	2.0° (a)	1.41° (b)	0.71	PE	42(a)
	(DA)		1.68° (b)	0.84		70(b)
<i>Chrysomyia</i>						
<i>megacephala</i> (♂)	NS	1.4°	1.37°	0.98	OE	81
<i>Apis mellifera</i>	A	1.7° (a)	2.6° (b)	1.53	PE	67(a)
						34(b)

^aEye types as in Table 1. (DA) and (LA), dark and light adapted. Methods: E, electrophysiology; P, pseudopupil; o, ophthalmoscopy.

the Lepidoptera and Coleoptera, apposition and superposition eyes (Figure 4) cover a similar range of values of $\Delta\phi$.

The relation between $\Delta\phi$ and the acceptance angle $\Delta\rho$ is of considerable interest because it indicates how the optical image is sampled. Recall that the finest grating frequency that the optics and the rhabdom can just resolve is equal to $1/\Delta\rho$ (Equation 8), and the finest frequency that the ommatidial array can transmit is equal to $1/(2\Delta\phi)$ (Equation 1). So in conditions where photon numbers are not limiting, one might expect $\Delta\rho$ to be twice $\Delta\phi$. If the ratio $\Delta\rho/\Delta\phi$ is less than 2 then the image can be said to be under-sampled, and if it is more then it is over-sampled. If the ratio is 2, then sampling is said to be matched, as it is in humans. Table 2 presents some recent studies in which both $\Delta\phi$ and $\Delta\rho$ have been measured accurately. In all but a few cases the $\Delta\rho/\Delta\phi$ is less than 2. The exceptions are all from dark-adapted or dark-

living animals (e.g. the mantid *Tenodera australasiae* in the dark, the nocturnal beetle *Anoplognathus pallidicollis*, the crepuscular butterfly *Melanitis leda* and the crepuscular beetle *Onitis alexis* ratios not far below 2 when dark-adapted). For the remainder of the light-adapted diurnal insects in the table, the average $\Delta\rho/\Delta\phi$ ratio is 1.07, implying undersampling. This will give high contrast in the image (around 0.4%) at the spatial sampling frequency of the ommatidial mosaic (Figure 3*b*). Why insects need this high contrast when humans do not is, however, unclear. One suggestion (73) is that flying insects rotate rapidly, and so the “real” values of $\Delta\rho$ are widened by motion blur (Equation 12). For a fly, rotation at a few hundred degrees per second would double the effective value of $\Delta\rho$ from 1.5 to 3° , resulting in the matched condition. The reason why in dark-living animals the ratio increases above 2 is presumably because a high value of $\Delta\rho$ is needed to increase the number of photons caught (Equation 11).

Departures from Uniform Symmetry

Most insect apposition eyes do not sample the surroundings in a uniform way. These nonuniformities are of two kinds. There are variations in local angular sampling density, giving some regions higher resolution than others, thereby creating acute zones (or “foveas”). There may also be differences between the spacing of ommatidial axes in the horizontal and vertical directions. Thus, to describe fully the way that the eye samples the environment, it is necessary to measure $\Delta\phi_h$ and $\Delta\phi_v$ (Figures 2*b*; see Figure 6) in all eye regions. The need for these asymmetries arises from the fact that insect eyes are cramped for space because of the limit to resolution imposed by diffraction (Equation 13). Acute zones have to be sneaked in at the expense of lower resolution elsewhere, and if there is less need for horizontal than for vertical acuity, space can be saved by appropriately distorting the pattern of ommatidial axes. Optical superposition eyes usually show less distortion than apposition eyes, because the optical system does not allow much departure from a spherical form.

There seem to be three broad patterns in the distribution of axes in apposition eyes (38): an overall pattern associated with forward flight, acute zones concerned with the capture of prey or mates, and horizontal acute strips associated with flat environments such as water surfaces (Figure 5). In describing these patterns it is helpful to indicate how intensively the ommatidial array samples different regions of the surroundings. The measure adopted in here is the number of ommatidial axes per square degree, or axis density (see section on acute zones). This is easily calculated as $1/(2\Delta\phi_h\Delta\phi_v)$, or $1/(\sqrt{3}\Delta\phi^2/2)$ if the array is symmetrical.

THE FORWARD FLIGHT PATTERN Bees, butterflies, and acridid grasshoppers are all flying herbivores, and share a characteristic and pronounced pattern of

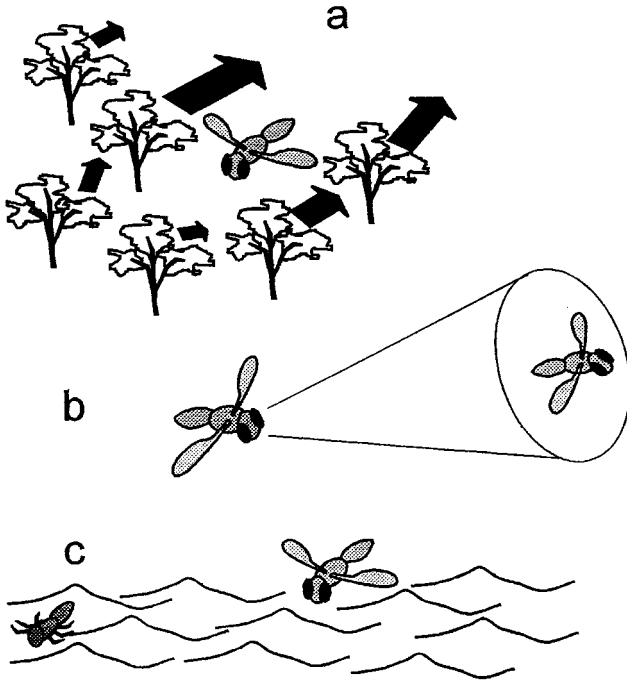


Figure 5 Three ecological situations that lead to variations in ommatidial axis densities across the eye. (a) Flight close to vegetation. The heavy black lines indicate the magnitude of the angular velocities in the flow-field across the insect's retina. (b) Pursuit. This typically requires an acute zone in the frontal or dorsal regions of the eyes. (c) Feeding above or below a flat surface, where all information of interest lies in a narrow band along the horizon.

changing interommatidial axis density and vertical/horizontal ratio across the eye. There are two separate gradients. The angle $\Delta\phi_h$ is smallest in the front of the eye and increases towards the back, and $\Delta\phi_v$ is smallest around the eye's equator, increasing towards both dorsal and ventral pole. This results in a frontal acute zone and a band around the equator with enhanced vertical, but not horizontal, acuity (38). This pattern was first noticed in bees and butterflies (3, 10), subsequently in locusts (1), and in various other insects (23, 38).

Figure 6 shows the pattern of ommatidial receptive fields in different regions of the eye of the Australian butterfly *Heteronympha merope*. The circles represent the dark-adapted acceptance angles ($\Delta\rho = 1.9^\circ$) measured optically (52), which vary little across the eye, as does the facet diameter (21–26 μm). There are, however, major variations in both $\Delta\phi_h$ and $\Delta\phi_v$. From the front horizontally to 120° , $\Delta\phi_h$ approximately doubles, pulling the vertical rows of axes

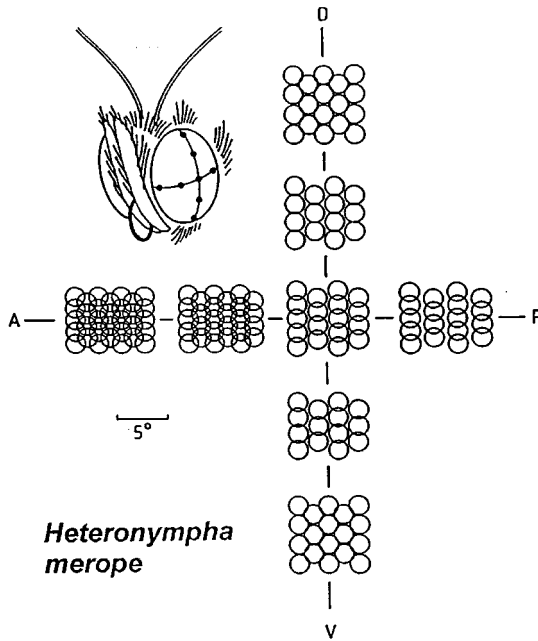


Figure 6 Patterns of ommatidial acceptance angles in different regions of the eye of the Australian woodland butterfly *Heteronympha merope*. A, D, P, V: anterior, dorsal, posterior and ventral.

apart. Vertically in either direction from the horizontal midline, $\Delta\phi_v$ increases by a third, separating the individual fields in the vertical rows.

A similar pattern has been documented in worker honey bees (38, 67). Here, the horizontal variation is smaller than that in butterflies, but the vertical variation is greater. The highest value for $\Delta\phi_h$ is not in the forward direction but is about 40° from the midline; this possibly is related to the amount of sideways maneuvering bees undertake compared to butterflies. Locusts and other acridid grasshoppers are intermediate between bees and butterflies. However, tettigoniid grasshoppers (bush crickets) that rarely fly have spherical eyes with none of these patterns of distortion (the author's personal observations). Female blowflies (*Calliphora erythrocephala*) also show a pattern similar to that in butterflies (42), although in the males this pattern is distorted to give a pronounced acute zone concerned with mate capture (Figure 7b).

What are the reasons for these gradients? The front-to-back acuity decrease is probably attributable to the motion flow-field encountered by insects in flight and to the blur that results from it (38). An insect flying in a straight line has a stationary view directly ahead but has a fast-moving field to the side,

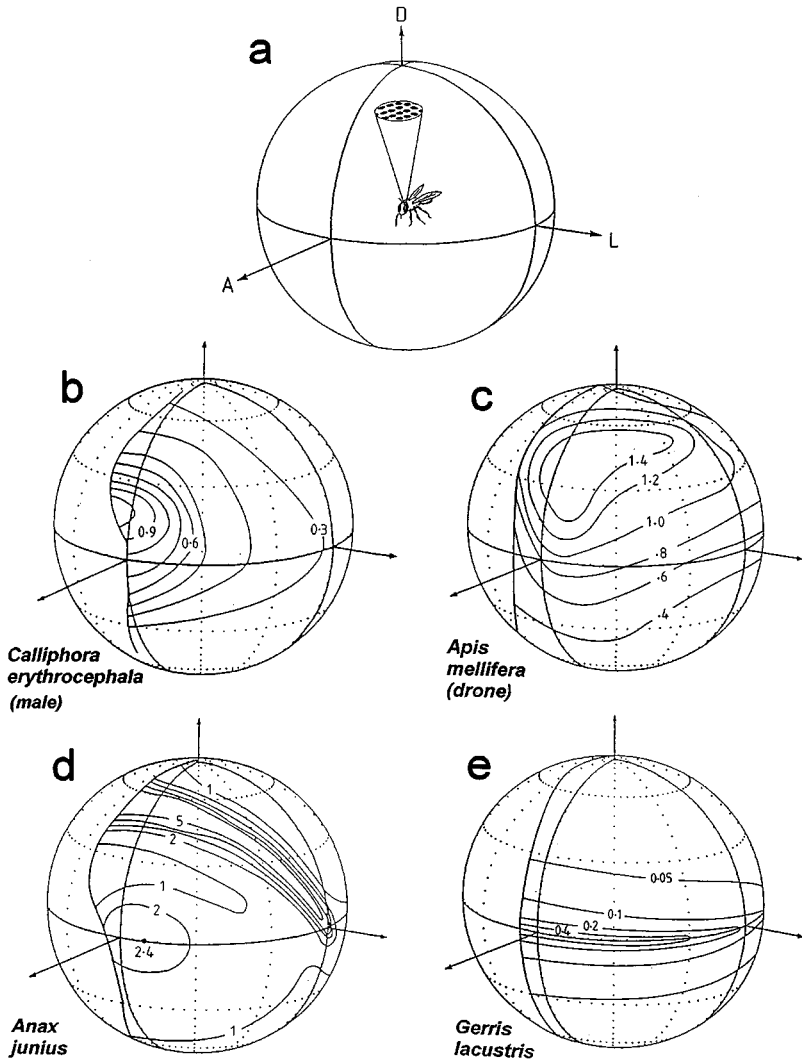


Figure 7 Distribution of ommatidial axis densities across the fields of view of four insects. (a) The meaning of axis density: the number of ommatidial axes per unit solid angle plotted onto a sphere around the insect. A, D, L: anterior, dorsal & lateral. Axis density plots shown are for (b) a male blowfly (data from 42), (c) a drone honey-bee (data from 67), (d) a dragonfly (data from 69), and (e) for a water strider (data from 8). Numbers are ommatidial axes per square degree.

particularly if it is flying close to vegetation (e.g. Figure 1 in Ref. 5). The relationship between image angular velocity v and the distance of an object b from the insect is given by the following:

$$v = \frac{U \sin \alpha}{b}, \quad (14)$$

where U is the insect's linear velocity, and α the angle between the object and the forward direction. For an insect flying near foliage, the resulting blur will roughly double the effective acceptance angle (Equation 12), which will "fill in" the horizontal rows in *H. merope* (Figure 6). For the vertical variations in $\Delta\phi_v$ there is no equivalent argument. Here the most likely reason for such variation is that there is more relevant detail in the region around the eye's equator, especially to an insect feeding on flowers, and hence the need for higher acuity in that part of the field. This "terrain hypothesis" is commonly used to explain the presence of "visual streaks" in vertebrate retinæ (26).

ACUTE ZONES CONCERNED WITH PREY CAPTURE AND MATING Many insects have a forward or upward-pointing region of high acuity. Where both sexes have the specialization (mantids, dragonflies, robber-flies), predation is the reason, but more commonly only the male has the acute zone (simuliid midges, hoverflies, mayflies, drone bees), implying use for sexual pursuit. In male houseflies and blowflies the acute zone may be little more than a local increase in the acuity of the "forward flight" acute zone common to both sexes (42). At the other extreme they may be separate eyes, as in the dorsal eyes of male bibionid flies (90) and the "turbanate" eyes of male mayflies (24), used for detecting females against the sky (32).

In male *C. erythrocephala* the acute zone lies 20–30° above the equator (Figure 7b) and is characterized by a lower value for $\Delta\phi$ than in the female (male 1.07°, female 1.28°) and larger facets (male 37 μm , female 29 μm) (42). In houseflies (*M. domestica*) and probably other flies the acute zone shows anatomical differences at the receptor level (19). Receptor R7, for example, sends its axon to the lamina rather than the medulla, a change seen as improving sensitivity slightly. Central to the lamina, a number of male-specific interneurons have been discovered, which are undoubtedly involved in the organization of pursuit behaviour (21, 74).

In the hoverfly *Syrirta pipiens* the sex difference is more striking (7). In the male's acute zone, $\Delta\phi$ is about three times smaller (0.6°) than anywhere in the female eye. A male uses this advantage to track a female while remaining beyond her visual detection range. Other Dipterans show a very wide variety of sex-specific acute zones, beautifully described by Dietrich (11). Drone bees have a similar anterodorsal acute zone, where the density of ommatidial axes

is three to four times greater than in the female eye (Figure 7c). They use this region when chasing the queen (as illustrated in experiments with a dummy queen on a string) (82). The minimum target size that a drone will pursue subtends 0.32° , which is much smaller than the ommatidial acceptance angle of 1.2° (77). Thus the trigger for pursuit is a brief decrease of about 6% in the intensity of background sky light received by single rhabdoms. This is one of the few good measurements available of the “single object threshold” of an insect eye. Simuliid flies also use the upper part of their divided eyes to detect potential mates against the sky, and they can do so at a distance of 0.5 m, when a female subtends an angle of only 0.2° , again a small fraction of an acceptance angle (31, 32). Tsetse flies (*Glossina morsitans*) seem to need a much larger signal to evoke chasing, about 1.6° across, which is similar to the foveal acceptance angle (4).

An increase in the detectability of small objects can be achieved either by reducing $\Delta\rho$, so that a small target causes a large change in the signal on the rhabdom that images it, or by increasing the numbers of photons available to the rhabdoms, thereby reducing the noise against which the signal must be detected. Either method requires a larger facet diameter D (Equation 7 and 11). In most known examples increases in facet diameter have evolved to reduce $\Delta\rho$. However, the male blowfly *Chrysomya megalcephala* has a “bright zone” rather than an acute zone, where $\Delta\rho$ is similar to the rest of the eye, but the photon catch per rhabdomere is enhanced roughly tenfold by an increase in both facet and rhabdomere diameter (81). Perhaps this enables the fly to mate in particularly dim conditions.

Although it is males that generally have acute zones, females of the pipunculid flies in the genus *Chalarus*, have greatly enlarged frontodorsal ommatidia (27). These flies parasitize leafhoppers, and the ovipositing females must locate these on the undersides of leaves. The males have no equivalent need for keen eyesight.

Dragonflies hunt other insects on the wing and have acute zones with a variety of configurations (23, 69). Many have two acute zones, one forward pointing (presumably concerned with forward flight as discussed above) and another directed dorsally for prey capture (Figure 7d). In perching libellulids the frontal zone is minimal, but there is an acute zone about 40° wide in the frontodorsal region. The migratory, fast-flying aeshnids have the largest eyes of all insects and among the most impressive acute zones. *Anax junius* has 28,672 ommatidia in each eye (69), and also has the smallest recorded interommatidial angles of any insect— 0.24° in the dorsal acute zone. This zone (Figure 7d) provides a narrow band of high resolution extending across both upper fields of view along a great circle. The axis density (5 per square degree) is five times higher than in male *Calliphora enthrocephala*. The dorsal acute zone is easily visible as a wedge of

enlarged facets (each 62 μm in diameter), although the forward-pointing zone is much less obvious. Presumably, the high-acuity stripe in *A. junius* is used to trawl through the air, picking out insects against the sky, much as the scan line on a radar screen picks up aircraft. Aeschnid larvae are also predatory, catching prey underwater. They too have an acute zone with low $\Delta\phi$ values (68), but it is frontal rather than dorsal. Little of the larval eye remains in the adult.

Like dragonfly larvae, praying mantids are ambush predators. They have large, binocularly overlapping acute zones that are used to center prey before it is struck with the spiked forelegs (61). Mantids, perhaps unique among insects, determine prey distance by binocular triangulation (62, 63). In *Tenodera australasiae*, Rossel (60) found that $\Delta\phi$ varied from 0.6° in the acute zone center to 2.5° laterally, and that in all regions of the eye $\Delta\rho$ was virtually identical to $\Delta\phi$ (Table 2). Facet diameters decreased from 50 μm in the acute zone to 35 μm peripherally, but this is less of a decrease than would be expected from diffraction considerations alone (Equation 4).

Although acute zones are nearly all frontal or dorsal, there are exceptions. Whiteflies (*Aleyrodes proletella*: Hemiptera) have divided eyes with larger facets ventrally (47); it is not known why. The situation in certain phorid flies is more comprehensible; they follow ants or termites by flying above them, prior to laying eggs on them (12). In the most extreme case (*Apocephalus laceyi*) the ventral facets are 35 μm across, and the dorsal ones 26 μm . In mosquitoes the lower facets are also larger (48), perhaps because of the need to see the ground during navigation in dim light.

HORIZONTAL ACUTE ZONES As we have seen, flying insects have increased vertical acuity around their eyes horizon, reflecting the visual importance of this region. There are environments where the horizon region is even more important, and eye design reflects this. Crabs that inhabit sand flats have a narrow band of high vertical acuity around the equators of the eyes (91), and ants (*Cataglyphis* sp. bicolor) that scavenge the desert surface also have a high acuity band around the horizon (92). Water surfaces provide a similarly restricted visual environment. Water-striders (*Gerris lacustris*) hunt prey stranded in the surface film and have a narrow acute band only about 10° high, imaging the horizon (Figure 7e). Within this acute band, $\Delta\phi_v$ in the frontal region is only 0.55° , but $\Delta\phi_h$ is 1.9° , and both $\Delta\phi_h$ and $\Delta\phi_v$ increase towards the rear (8). These insects have an open rhabdom eye and probably have some form of neural superposition, as in Diptera (8, 50).

The backswimmer (*Notonecta glauca*) is in some ways more remarkable. It hangs inverted from the surface, so that it looks upwards with what is morphologically the ventral part of the eye. Its typical prey consists of insects struggling in the surface film, and it actually has two views of them. If it looks

upward at about 48° from the vertical it will look out into air, but the line of sight, after refraction, lies along the surface. If it looks lower $60\text{--}70^\circ$ down from the vertical, it will also view the surface, but this time from below, through the water. Schwind (65) found that *N. glauca* has two acute bands across its eyes that correspond to the images of these two views of the surface, both of which look into the direction of potential prey. In each band $\Delta\phi$ is $1\text{--}2^\circ$, with a lower acuity zone between them where $\Delta\phi$ falls to 4° .

Empid flies also inhabit the water surface, but they fly just above it, searching for drowning insect prey. Some (*Hilaria* and *Rhamphomyia* spp.) have a pronounced band of enlarged facets around the eye equator and a corresponding 20° high acute region; presumably the large facets here serve to improve the diffraction limit (Equation 4). Vertical resolution increases by a factor of 3–4 in the acute band (91).

CONCLUDING REMARKS

The preceding examples show how well the insect compound eye can adapt to different environmental conditions by subtle changes in its structure. As Walls remarked in his great book on the vertebrate eye (84a): “Everything in the vertebrate eye means something;” and this is just as true of insect eyes. The variations in facet diameter, in optical construction, in the angles between ommatidia, and in rhabdom diameter and length all allow the eye to make the most of the information in the environment. This is in spite of the fact that the tiny lenses of compound eyes severely limit resolution. Nilsson has put it very well (49): “It is only a small exaggeration to say that evolution seems to be fighting a desperate battle to improve a basically disastrous design.” One of the intriguing unsolved problems of insect vision is why this design persisted when alternatives were apparently at hand, in the form of dorsal and larval ocelli, both of which have a single lens construction (36). Either there is something we still do not know about compound eyes, or evolution is remarkably conservative on some occasions.

Literature Cited

1. Autrum H, Wiedemann I. 1962. Versuche über den Strahlengang im Insektenauge. *Z. Naturforsch.* 17b:480–82
2. Barlow HB. 1952. The size of ommatidia in apposition eyes. *J. Exp. Biol.* 29:667–74
3. Baumgärtner H. 1928. Der Formensinn und die Sehschärfe der Bienen. *Z. Vergl. Physiol.* 7:56–143
4. Brady J. 1991. Flying mate detection and chasing by tsetse flies (*Glossina*). *Physiol. Entomol.* 16:153–61
5. Buchner E. 1984. Behavioural analysis of spatial vision in insects. In *Photoreception and Vision in Invertebrates*, ed. MA Ali, pp. 561–621. New York: Plenum
6. Cleary P, Deichsel G, Kunze P. 1977. The superposition image in the eye of *Ephesia kühniella*. *J. Comp. Physiol. A* 119:73–84
7. Collett TS, Land MF. 1974. Visual control

- of flight behaviour in the hoverfly *Syrirta pipiens* L. *J. Comp. Physiol.* 99:1–66
8. Dahmen H. 1991. Eye specialisation in waterstriders: an adaptation to life in a flat world. *J. Comp. Physiol. A* 169:623–32
 9. de Vries H. 1956. Physical aspects of the sense organs. *Prog. Biophys.* 6:207–64
 10. del Portillo J. 1936. Beziehungen zwischen den Öffnungswinkeln der Ommatidien, Krümmung und Gestalt der Insektenaugen und ihrer funktionellen Aufgabe. *Z. Vergl. Physiol.* 23:100–45
 11. Dietrich W. 1909. Die Facettenaugen der Dipteren. *Z. Wiss. Zool.* 92:465–539
 12. Disney RHL, Schroth M. 1989. Observations on *Megaselia persecutrix* Schmitz (Diptera: Phoridae) and the significance of ommatidial size-differentiation. *Entomol. Mon. Mag.* 125:169–174
 13. Exner S. 1891. *Die Physiologie der facettierten Augen von Krebsen und Insecten*. Leipzig: Deuticke. Transl. R Hardie. 1989. *The Physiology of the Compound Eyes of Insects and Crustaceans*. Berlin: Springer
 14. Franceschini N. 1975. Sampling of the visual environment by the compound eye of the fly: fundamentals and applications. In *Photoreceptor Optics*, ed. AW Snyder, R Menzel, pp. 98–125. Springer: Berlin
 15. Franceschini N, Kirschfeld K. 1971. Les phénomènes des pseudopupille dans l'oeil de *Drosophila*. *Kybernetik* 9:159–182
 16. Götz KG. 1965. Die optischen Übertragungseigenschaften der Komplexaugen von *Drosophila*. *Kybernetik* 2:215–221
 17. Hardie RC. 1979. Electrophysiological analysis of the fly retina. I. Comparative properties of R1–6 and R7 and R8. *J. Comp. Physiol. A* 129:19–33
 18. Hardie RC. 1984. Functional organization of the fly retina. *Prog. Sens. Physiol.* 5:1–79
 19. Hardie RC, Franceschini N, Ribi W, Kirschfeld K. 1981. Distribution and properties of sex-specific photoreceptors in the fly *Musca domestica*. *J. Comp. Physiol. A* 145:139–52
 20. Hassenstein B. 1951. Ommatidiensraster und afferente Bewegungsintegration. (Versuche an dem Rüsselkäfer *Chorophanus viridis*) *Z. Vergl. Physiol.* 33:301–26
 21. Hausen K, Strausfeld N. 1980. Sexually dimorphic interneuron arrangements in the fly visual system. *Proc. R. Soc. London B* 208:51–71
 22. Horridge GA. 1969. The eye of the firefly *Photuris*. *Proc. R. Soc. London B* 171:445–63
 23. Horridge GA. 1978. The separation of visual axes in apposition compound eyes. *Phil. Trans. R. Soc. London B* 285:1–59
 24. Horridge GA, McLean M. 1978. The dorsal eye of *Atalophlebia* (Ephemeroptera). *Proc. R. Soc. London B* 200:137–50
 25. Howard J, Dubs A, Payne R. 1984. The dynamics of phototransduction in insects. A comparative study. *J. Comp. Physiol. A* 154:707–18
 26. Hughes A. 1977. The topography of vision in mammals of contrasting lifestyle: comparative optics and organization. In *Handbook of Sensory Physiology, Vol. VII/5*, ed. F Crescitelli, pp. 613–756. Berlin: Springer
 27. Jervis MA. 1992. A taxonomic revision of the pipunculid fly genus *Chalarus* Walker, with particular reference to the European fauna. *Zool. Linn. Soc.* 105:243–52
 28. Kirschfeld K. 1967. Die Projektion der optischen Umwelt auf das Raster der Rhabdome im Komplexauge von *Musca*. *Exp. Brain. Res.* 3:248–70
 29. Kirschfeld K. 1974. The absolute sensitivity of lens and compound eyes. *Z. Naturforsch.* 29c:592–96
 30. Kirschfeld K. 1976. The resolution of lens and compound eyes. In *Neural Principles in Vision*, ed. F Zettler, R Weiler, pp. 354–70. Berlin: Springer
 31. Kirschfeld K. 1979. The visual system of the fly: physiological optics and functional anatomy as related to behaviour. In *The Neurosciences 4th Study Program*, ed. FO Schmitt, FG Worden, pp. 297–310. Cambridge, Mass: MIT Press
 32. Kirschfeld K, Wenk P. 1976. The dorsal compound eye of simuliid flies: an eye specialized for the detection of small, rapidly moving objects. *Z. Naturforsch.* 31c:764–65
 33. Kunze P. 1979. Apposition and superposition eyes. In *Handbook of Sensory Physiology, Vol. VII/6A*, ed. H Autrum, pp. 442–502. Berlin: Springer
 34. Labhart T. 1980. Specialized photoreceptors at the dorsal rim of the honeybee's compound eye: polarizational and angular sensitivity. *J. Comp. Physiol. A* 141:19–30
 35. Labhart T, Nilsson D-E. 1995. The dorsal eye of the dragonfly *Sympetrum*: specializations for prey detection against the sky. *J. Comp. Physiol. A* 176:437–53
 36. Land MF. 1981. Optics and vision in invertebrates. In *Handbook of Sensory*

- Physiology, Vol. VII/6B*, ed. H. Autrum, pp. 472–592. Berlin: Springer
37. Land MF. 1984. The resolving power of diurnal superposition eyes measured with an ophthalmoscope. *J. Comp. Physiol. A* 154:515–33
 38. Land MF. 1989. Variations in the structure and design of compound eyes. In *Facets of Vision*, ed. DG Stavenga, R Hardie, pp. 90–111. Berlin: Springer
 39. Land MF. 1990. Direct observation of receptors and images in simple and compound eyes. *Vision Research* 30:1721–34
 40. Land MF. 1993. The visual control of courtship in the fly *Poecilobothrus nobilitatus*. *J. Comp. Physiol. A* 173:595–603
 41. Land MF. 1994. The functions of eye movements in animals remote from man. In *Eye Movement Research*, ed. JA Findlay, R Walker, RW Kenridge, pp. 63–76. Amsterdam: Elsevier
 42. Land MF, Eckert H. 1985. Maps of the acute zones of fly eyes. *J. Comp. Physiol. A* 156:525–38
 43. Land MF, Osorio D. 1990. Waveguide modes and pupil action in the eyes of butterflies. *Proc. R. Soc. London B* 241:93–100
 44. Laughlin SB. 1974. Neural integration in the first optic neuropile of dragonflies. III. The transfer of angular information. *J. Comp. Physiol. A* 92:377–96
 45. Laughlin SB, Weckström M. 1993. Fast and slow photoreceptors—a comparative study of the functional diversity of coding and conductances in the Diptera. *J. Comp. Physiol. A* 172:593–609
 46. Mallock A. 1894. Insect sight and the defining power of compound eyes. *Proc. R. Soc. London B* 55:85–90
 47. Mallock A. 1922. Divided composite eyes. *Nature (London)* 110:770–71
 48. Mazokhin-Porschnyakov GA. 1969. *Insect Vision*. New York: Plenum
 49. Nilsson D-E. 1989. Optics and evolution of the compound eye. In *Facets of Vision*, ed. DG Stavenga, RC Hardie, pp. 30–75. Berlin: Springer
 50. Nilsson D-E, Ro A-I. 1994. Did neural pooling for night vision lead to the evolution of neural superposition eyes? *J. Comp. Physiol. A* 175:289–302
 51. Nilsson D-E, Land MF, Howard J. 1984. Afocal apposition optics in butterfly eyes. *Nature (London)* 312:561–63
 52. Nilsson D-E, Land MF, Howard J. 1988. Optics of the butterfly eye. *J. Comp. Physiol. A* 162:341–66
 53. Pask C, Barrell KF. 1980. Photoreceptor optics I: Introduction to formalism and excitation in a lens-photoreceptor system. *Biol. Cybern.* 36:1–8
 54. Pask C, Barrell KF. 1980b. Photoreceptor optics II: Application to angular sensitivity and other properties of a lens-photoreceptor system. *Biol. Cybern.* 36:9–18
 55. Paulus H. 1975. The compound eye of apterygote insects. In *The Compound Eye and Vision of Insects*, ed. GA Horridge, pp. 1–20. Oxford: Clarendon
 56. Pelli DG. 1990. The quantum efficiency of vision. In *Vision: Coding and Efficiency*, ed. C Blakemore, pp. 3–24. Cambridge: Cambridge Univ. Press
 57. Pirenne MH. 1967. *Vision and the Eye*. London: Chapman & Hall
 58. Reichardt W. 1966. Quantum sensitivity of light receptors in the compound eye of the fly *Musca*. *Cold Spring Harbor Symp. Quant. Biol.* 30:505–15
 59. Rose A. 1972. *Vision: Human & Electronic*. New York: Plenum
 60. Rossel S. 1979. Regional differences in photoreceptor performance in the eye of the praying mantis. *J. Comp. Physiol.* 131:95–112
 61. Rossel S. 1980. Foveal fixation and tracking in the praying mantis. *J. Comp. Physiol.* 139:307–31
 62. Rossel S. 1983. Binocular stereopsis in an insect. *Nature (Lond.)* 302:821–22
 63. Rossel S. 1991. Spatial vision in the praying mantis: Is distance implicated in size perception? *J. Comp. Physiol. A* 169:101–8
 64. Schneider L, Gogala M, Draslar K, Langer H, Schlecht P. 1978. Feinstruktur und Schirmpigment-Eigenschaften der Ommatidien des Doppelauges von *Ascalaphus* (Insecta, Neuroptera). *Cytobiologie* 16:274–307
 65. Schwind R. 1980. Geometrical optics of the *Notonecta* eye: adaptations to optical environment and way of life. *J. Comp. Physiol.* 140:59–68
 66. Seidl R. 1980. Die Sehfelder und Ommatidien-Divergenzwinkel der drei Kasten der Honigbiene (*Apis mellifica*). *Verh. Dtsch. Zool. Ges.* 1980, 367. Stuttgart: Gustav Fischer
 67. Schwind R. 1982. *Die Sehfelder und Ommatidien-Divergenzwinkel von Arbeiterin, Königin und Drohne der Honigbiene (Apis mellifica)*. PhD thesis. Darmstadt: Tech Hochsch. Darmstadt
 68. Sherk TE. 1977. Development of the compound eyes of dragonflies. I. Larval compound eyes. *J. Exp. Zool.* 201:391–416
 69. Sherk TE. 1978. Development of the compound eyes of dragonflies. III. Adult

- compound eyes. *J. Exp. Zool.* 203:61–80
70. Smakman JGJ, Hateren JH, Stavenga DG. 1984. Angular sensitivity of blowfly photoreceptors: intracellular measurements and wave-optical predictions. *J. Comp. Physiol. A* 155:239–47
 71. Snyder AW. 1975. Photoreceptor optics—theoretical principles. In: *Photoreceptor Optics*, ed. AW Snyder, R Menzel, pp. 38–55. Berlin: Springer
 72. Snyder AW. 1977. Acuity of compound eyes: physical limitations and design. *J. Comp. Physiol.* 116:161–82
 73. Snyder AW. 1979. Physics of vision in compound eyes. In *Handbook of Sensory Physiology, Vol. VII/6A*, ed. H Autrum, pp. 225–313. Berlin: Springer
 74. Strausfeld NJ. 1991. Structural organization of male-specific visual neurons in caliphorid optic lobe. *J. Comp. Physiol. A* 169:379–93
 75. Srinivasan MV, Lehrer M. 1988. Spatial acuity of honeybee vision and its spectral properties. *J. Comp. Physiol. A* 162: 159–72
 76. Stavenga DG. 1979. Pseudopupils of compound eyes. In *Handbook of Sensory Physiology, Vol. VII/6A*, ed. H Autrum, pp. 357–439. Berlin: Springer
 77. Vallet AM, Coles JA. 1991. A method of estimating the minimum visual stimulus that evokes a behavioural response in the drone, *Apis mellifera* male. *Vision Res.* 31:1453–55
 78. van Hateren JH. 1984. Waveguide theory applied to optically measured angular sensitivities of fly photoreceptors. *J. Comp. Physiol. A* 154:761–71
 79. van Hateren JH. 1989. Photoreceptor optics: theory and practice. In *Facets of Vision*, ed. DG Stavenga, RC Hardie, pp. 74–89. Berlin: Springer
 80. van Hateren JH, Nilsson D-E. 1987. Butterfly optics exceed the theoretical limits of conventional apposition eyes. *Biol. Cybern.* 57:159–68
 81. van Hateren JH, Hardie RC, Rudolph A, Laughlin SB, Stavenga DG. 1989. The bright zone, a specialised dorsal eye region in the male blowfly *Chrysomya megalocephala*. *J. Comp. Physiol. A* 164:297–308
 82. van Praagh JP, Ribl W, Wehrhahn C, Wittmann D. 1980. Drone bees fixate the queen with the dorsal frontal part of their compound eyes. *J. Comp. Physiol.* 136:263–66
 83. von Buddenbrock W. 1952. *Vergleichende Physiologie Bd I. Sinnesphysiologie*. Basel: Birkhäuser
 84. Via SE. 1977. Visually mediated snapping in the bulldog ant: a perceptual ambiguity between size and distance. *J. Comp. Physiol.* 121:33–51
 - 84a. Walls GL. 1942. *The Vertebrate Eye and its Adaptive Radiation*. Bloomfield Hills, Michigan: Cranbrook Inst.
 85. Warrant EJ, McIntyre PD. 1990. Limitations to resolution in superposition eyes. *J. Comp. Physiol. A* 167:785–803
 86. Warrant EJ, McIntyre PD. 1993. Arthropod eye design and the physical limits to spatial resolving power. *Prog. Neurobiol.* 40:413–61
 87. Wehner R. 1981. Spatial vision in arthropods. In *Handbook of Sensory Physiology, Vol. VII/6C*, ed. H Autrum, pp. 287–616. Springer: Berlin
 88. Williams DS. 1983. Changes of photoreceptor performance associated with the daily turnover of photoreceptor membrane in locusts. *J. Comp. Physiol.* 150:509–19
 89. Woodhouse JM, Barlow HB. 1982. Spatial and temporal resolution and analysis. In *The Senses*, ed. HB Barlow, JD Mollon, pp. 133–64. Cambridge: Cambridge Univ. Press
 90. Zeil J. 1983. Sexual dimorphism in the visual system of flies: the compound eyes and neural superposition in Bibionidae (Diptera). *J. Comp. Physiol.* 150:379–93
 91. Zeil J, Nalbach G, Nalbach H-O. 1989. Spatial vision in a flat world: optical and neural adaptations in arthropods. In *Neurobiology of Sensory Systems*, ed. RN Singh, NJ Strausfeld, pp. 123–37. New York: Plenum
 92. Zollikofer CPE, Wehner R, Fukushi T. 1995. Optical scaling in conspecific *Cataglyphis* ants. *J. Exp. Biol.* 198:1637–46